# Role of baryon resonances in the $\pi^- p \to n e^+ e^-$ reaction within an effective-Lagrangian model

Miklós Zétényi *
*Wigner Research Centre for Physics, Budapest, Hungary*

Deniz Nitt and Michael Buballa
*Technische Universität Darmstadt, Department of Physics, Darmstadt, Germany*

Tetyana Galatyuk
*Technische Universität Darmstadt, Department of Physics, Darmstadt, Germany*
*and GSI Helmholtzzentrum für Schwerionenforschung GmbH, Darmstadt, Germany*

(Received 22 December 2020; accepted 24 June 2021; published 23 July 2021)

We present a study of the reaction $\pi^- p \to n e^+ e^-$ for $\sqrt{s} = 1.49$ GeV, including nonresonant Born terms and contributions of the $N(1440)$, $N(1520)$, $N(1535)$ resonances (R), using an effective-Lagrangian model, which we extended by a phenomenological phase factor at the R$N\rho$ vertex function. We give predictions for both the differential cross section $d\sigma/dm_{\rm inv}$ and the spin density matrix elements of the virtual photon that decays into the lepton pair. In the studied energy range, the cross section is dominated by the Born and $N(1520)$ contributions.

DOI: 10.1103/PhysRevC.104.015201

## I. INTRODUCTION

Electromagnetic probes (photons and correlated lepton-antilepton pairs, called dileptons) provide a unique tool to study properties of strongly interacting matter [1–3]. Once produced in pion-, proton-, or nucleus-nucleus collisions, photons and dileptons leave the interaction volume essentially unaffected by final-state interactions. Thus they preserve information about the medium they were created in, including the matter present in the hot and/or dense stage of the reaction [4–8]. In the low-mass region ($m_{\rm inv} < 1$ GeV), excess dileptons are radiated from channels involving baryons [9–13]. A strong broadening of the $\rho$ meson has been observed in experiments spanning from a few GeV to few TeV energy range. This trend hints at a strong coupling of the $\rho$ meson to baryonic resonances, being manifestations of in-medium modifications of vector mesons [14]. A determination of the couplings of baryonic resonances to final states involving dileptons is particularly important for the understanding of the dilepton emissivity of hot and dense nuclear matter.

Dileptons produced in hadronic processes test the electromagnetic interaction of hadrons in a kinematical domain inaccessible in electro- or photoproduction experiments. In pion-nucleon collisions, an important contribution is given by processes where a baryon resonance is excited and subsequently decays into the final-state particles. The resulting dilepton spectrum gives access to electromagnetic transition form factors of these baryon resonances in the timelike region. These form factors have been studied for the case of $\Delta(1232)$, $N(1520)$ and $N(1535)$ in the framework of the covariant spectator quark model which takes into account contributions from the valence quark core and the meson cloud [15–17].

The angular distribution of the lepton pair reflects the polarization state of the virtual photon, which in turn is determined by the hadronic reaction in which it was created [18]. Neutral vector mesons have the same quantum numbers as photons, therefore they can convert to a virtual photon. According to the vector-meson dominance (VMD) hypothesis [19], an essential contribution to the electromagnetic interaction of hadrons proceeds through an intermediate neutral vector meson, whose properties can be studied in the dilepton invariant-mass spectrum.

The HADES collaboration has recently carried out experiments using secondary pions impinging on polyethylene and carbon targets. The beam was provided by the SIS18 heavy-ion synchrotron at GSI in Darmstadt, Germany. The results are extracted for the $\pi^- p$ reaction at the center-of-mass (c.m.) energy of $\sqrt{s} = 1.49$ GeV, which lies in the second resonance region. HADES results for pion-pair production in $\pi^- p$ collisions are presented in Ref. [20]. The $\rho$ meson, which predominantly decays to a pion pair, contributes strongly to the reaction $\pi^- p \to n\pi^+\pi^-$. Similarly to dileptons, the angular distribution of the pion pair reflects the polarization state of the decaying $\rho$ meson.

In this paper we present a model calculation of the dilepton production process in pion-nucleon collisions at the c.m. energy of $\sqrt{s} = 1.49$ GeV. We give predictions for the invariant-mass spectrum of dielectrons. We also point out how the spin density matrix of the virtual photon could be reconstructed based on the angular distribution of lepton pairs. Our studies are based on the previous models used in Refs. [18,21].

*zetenyi.miklos@wigner.hu

 

In Ref. [21] the reaction $\pi^- p \to n e^+ e^-$ was studied in an effective-Lagrangian model taking into account both the contributions with baryon resonances in the $s$ and $u$ channels, and the nonresonant (Born) terms. Form factors were included for both the resonance and the Born contributions. A version of the VMD model was employed where electromagnetic interactions of hadrons can proceed both via an intermediate $\rho$ meson and a direct coupling to the photon field. Predictions for the dilepton invariant-mass spectrum were presented for various beam energies.

In Ref. [18] the focus was on the angular distribution of dileptons, which was studied in terms of anisotropy coefficients. The main conclusion was that the angular distribution of dileptons is characteristic of the creation process, in particular the spin-parity of intermediate baryon resonances. In that study, Born contributions were not considered, while interactions of higher-spin baryons were treated according to the consistent interaction scheme described in Ref. [22].

In the present calculation, we describe baryon resonances in the same way as in Ref. [18]. We include Born contributions and employ form factors as described in Ref. [21]. We extended the models by including a phenomenological phase factor in the Lagrangians describing the resonance transition to a nucleon and $\rho$ meson. This factor influences the numerical predictions of the model via interference effects.

The reaction $\pi N \to N e^+ e^-$ was studied for the energy range around the $\omega$ meson production threshold in terms of an effective Lagrangian model in Ref. [23] and in terms of a coupled-channel approach where baryon resonances were generated dynamically in Ref. [24]. In Ref. [23] the dominance of resonant contributions was assumed and the interaction Lagrangians of Ref. [25] were used. Both works discussed the effects of $\rho$-$\omega$ interference.

We also note that anisotropy of dilepton emission as a probe for polarization and a means of disentangling different contributions was first studied in hadron reactions in Ref. [26], and in nuclear collisions in Ref. [27].

More details about our model will be given in Sec. II and in the Appendix. Our results will be presented in Sec. III. Finally, in Sec. IV, we draw our conclusions and discuss possible future directions.

## II. MODEL

In this section, we briefly review the main elements of the applied models and outline the calculation of the observables. For further details the interested reader is referred to Refs. [18,21].

### A. Kinematics and observables

The differential cross section of the process $\pi^- p \to n e^+ e^-$ is given by

$$\frac{d\sigma}{dm_{\rm inv} d\cos\theta_{\gamma^*} d\Omega_e} = \frac{m_{\rm inv}}{64(2\pi)^4 s} \frac{|\mathbf{p}_f|}{|\mathbf{p}_i|} \frac{1}{n_{\rm pol}} \sum_{\rm pol} |\mathcal{M}|^2, \quad (1)$$

where $m_{\rm inv}$ denotes the mass of the virtual photon (= invariant mass of the $e^+e^-$ pair), $\theta_{\gamma^*}$ is the virtual-photon angle in the c.m. frame with respect to the pion-beam direction, i.e., the scattering angle, $d\Omega_e$ is the solid angle of the final-state electron given in the dilepton c.m. frame, $s$ is the square of the c.m. energy, $\mathbf{p}_i$ and $\mathbf{p}_f$ are the c.m. three-momenta of the incoming and outgoing nucleon, respectively, and $n_{\rm pol} = 2$ is the number of polarization states in the incoming channel. The sum runs over the polarization states of all incoming and outgoing particles.

Assuming that the virtual photon and final-state nucleon do not interact with each other, we can separate the hadronic and leptonic parts of the process by cutting the Feynman diagrams at the virtual photon line. The spin averaged squared amplitude can then be calculated as

$$\sum_{\rm pol} |\mathcal{M}|^2 = \sum_{\lambda,\lambda'} \rho^{\rm had}_{\lambda\lambda'} \rho^{\rm lep}_{\lambda'\lambda} \quad (2)$$

with the spin density matrices as introduced in Ref. [18],

$$\rho^{\rm had}_{\lambda,\lambda'}(s, m_{\rm inv}, \theta_{\gamma^*}) = \frac{e^2}{k^4} \epsilon_\mu(k,\lambda) W^{\mu\nu} \epsilon^*_\nu(k,\lambda'), \quad (3)$$

$$\rho^{\rm lep}_{\lambda',\lambda}(m_{\rm inv}, \Omega_e) = \epsilon_\mu(k,\lambda') l^{\mu\nu} \epsilon^*_\nu(k,\lambda), \quad (4)$$

describing the two subprocesses. The tensors $W^{\mu\nu} = \sum_{\rm pol} \mathcal{M}^\mu_{\rm had} \mathcal{M}^{\nu *}_{\rm had}$ and $l^{\mu\nu} = \sum_{\rm pol} \mathcal{M}^\mu_{\rm lep} \mathcal{M}^{\nu *}_{\rm lep}$ are related to the hadronic and the leptonic part of the amplitude, respectively, with $\mathcal{M}^\mu_{\rm had}$ and $\mathcal{M}^\mu_{\rm lep}$ denoting the corresponding transition currents. The virtual photon is characterized by its four-momentum $k$ and polarization $\lambda$, which also enter the polarization vector $\epsilon_\mu(k,\lambda)$.

As pointed out in Ref. [18], the form of $\rho^{\rm lep}_{\lambda',\lambda}$ can be calculated from quantum electrodynamics, therefore the angular distribution of $e^+e^-$ pairs can be expressed in terms of the hadronic density matrix elements. Making use of the Hermiticity of $\rho^{\rm had}_{\lambda,\lambda'}$ we obtain for the squared amplitude

$$\begin{aligned}\sum_{\rm pol} |\mathcal{M}|^2 \propto\ & (1+\cos^2\theta_e)\left(\rho^{\rm had}_{1,1} + \rho^{\rm had}_{-1,-1}\right) + 2\sin^2\theta_e \rho^{\rm had}_{0,0} \\ & + \sqrt{2}\sin 2\theta_e \left[\cos\phi_e \left(\mathrm{Re}\,\rho^{\rm had}_{1,0} - \mathrm{Re}\,\rho^{\rm had}_{-1,0}\right)\right. \\ & \left. + \sin\phi_e \left(\mathrm{Im}\,\rho^{\rm had}_{1,0} + \mathrm{Im}\,\rho^{\rm had}_{-1,0}\right)\right] \\ & + 2\sin^2\theta_e \left(\cos 2\phi_e\, \mathrm{Re}\,\rho^{\rm had}_{1,-1} + \sin 2\phi_e\, \mathrm{Im}\,\rho^{\rm had}_{1,-1}\right), \end{aligned} \quad (5)$$

see Eq. (15) in Ref. [18]. This makes it possible, at least in principle, to determine the hadronic density-matrix elements $\rho^{\rm had}_{\lambda,\lambda'}$ based on the angular distribution of the $e^+e^-$ pairs obtained in the experiments.

### B. Vector-meson dominance and effective Lagrangian

The vector-meson dominance model (VMD) was initially proposed by Sakurai to describe the coupling of a photon to a hadronic current via an intermediate vector meson [19,28]. We employ the later version of the VMD as discussed in Ref. [29], which also allows for a direct coupling of hadrons to the electromagnetic field. The Lagrangian of this version of VMD can be symbolically written as

$$\mathscr{L}_{\rm VMD} = -\frac{e}{2g_\rho} F^{\mu\nu} \rho^0_{\mu\nu} + \sum_{v,w} (\mathscr{L}_{\gamma vw} + \mathscr{L}_{\rho vw}), \quad (6)$$

TABLE I. Resonances and their parameters presented in this paper.

| | $m$ [GeV] | $\Gamma$ [GeV] | BR[a]$\to N\pi$ [%] | $g_{\pi NR}$ | BR[b]$\to N\rho$ [%] | $g_{\rho NR}$ | BR[a]$\to N\gamma$ [%] | $g_{\gamma NR}$ |
|---|---|---|---|---|---|---|---|---|
| $N(1440)$ | 1.440 | 0.350 | 55 – 75 | 0.38 | <0.2 | 3.37 | 0.02 – 0.04 | 0.053 |
| $N(1520)$ | 1.520 | 0.110 | 55 – 65 | 0.15 | $12.2 \pm 1.9$ | 13.9 | 0.30 – 0.53 | 0.36 |
| $N(1535)$ | 1.530 | 0.150 | 32 – 52 | 0.16 | $3.2 \pm 0.7$ | 1.97 | 0.01 – 0.25 | 0.058 |

[a]Taken from Ref. [32].
[b]Taken from Ref. [20].

where $F_{\mu\nu} = \partial_\mu A_\nu - \partial_\nu A_\mu$ and $\rho^0_{\mu\nu} = \partial_\mu \rho^0_\nu - \partial_\nu \rho^0_\mu$ are the field-strength tensors of the photon and neutral $\rho$ meson, respectively, expressed in terms of the corresponding fields. (In $\rho^0_{\mu\nu}$ we omitted the term quadratic in the $\rho$ field because it does not contribute to the process we study.)

The first term in Eq. (6) describes the $\rho$-$\gamma$ transition and its coupling constant is controlled by the parameter $g_\rho = 4.96$. The summation in the second term runs over pairs of hadron fields $v$, $w$, and the two symbolic terms represent both the interaction of various hadrons with the photon and the $\rho$ meson, like, e.g., $\mathscr{L}_{\gamma\pi\pi}$ or $\mathscr{L}_{\rho NN}$, and transition vertices of baryon resonances (R), like $\mathscr{L}_{\rho NR}$.

According to the other version of VMD,

$$\mathscr{L}'_{\rm VMD} = -\frac{e m_\rho^2}{g_\rho} A^\mu \rho^0_\mu + \sum_{v,w} \mathscr{L}'_{\rho vw}, \tag{7}$$

hadrons couple to the electromagnetic field only via an intermediate neutral vector meson. As pointed out in Refs. [28,30], the models $\mathscr{L}_{\rm VMD}$ and $\mathscr{L}'_{\rm VMD}$ are equivalent in the limit when all hadrons couple to the $\rho$ meson with the same universal coupling constant, which is equal to the parameter $g_\rho$ appearing in the denominator of the term describing the $\rho$-$\gamma$ transition in Eqs. (6) and (7), $g_{\rho\pi\pi} = g_{\rho NN} = \ldots = g_\rho$. In our model this universality does not hold, but the relative signs of the photon and $\rho$ meson interaction Lagrangians can be fixed based on the requirement that the two versions of VMD become equivalent when all the $\rho$ meson coupling constants approach a universal value.

For the nonresonant contributions we use the effective Lagrangians of Ref. [21]. The coupling of baryon resonances to the pion, $\rho$-meson, and photon fields are described by the effective-Lagrangian model from Ref. [18], where a consistent treatment of higher-spin contributions according to Ref. [22] has been taken care of. An important difference between the present model and the models of Refs. [18,21] is that here we fix the relative sign of hadron–photon and hadron–$\rho$-meson interaction terms based on the equivalence of the two versions of VMD in the universality limit, as discussed above. In Appendix A we list all terms of the effective Lagrangian applied in the present model. In principle, the VMD allows for all neutral vector mesons to couple between the hadronic current and the photon. Here, we only consider the contribution of the $\rho^0$ meson.

For those terms in the effective Lagrangian that do not contain baryon resonances we adopt the coupling constants from Ref. [21]. For the resonant contributions we need to fix the coupling constants $g_{\rho NR}$, $g_{\gamma NR}$, and $g_{\pi NR}$ individually. This has been done by calculating the corresponding partial decay width of the resonance and fitting it to the experimental value. Details are specified in Appendix B. Properties of baryon resonances, including the coupling constants are given in Table I.

### C. Hadronic processes

We consider the contributions shown in Fig. 1 for the hadronic part of the process. These include the nonresonant $s$-, $u$-channel diagrams, the $t$-channel with an intermediate pion, together with the contact term [Figs. 1(a)–1(d)] and the diagrams with $s$- and $u$-channel baryon resonances [Figs. 1(e) and 1(f)]. Each diagram in Fig. 1 is a sum of a direct photon and a $\rho$ meson contribution.

At $\sqrt{s} = 1.49\,\text{GeV}$, the nearby baryon resonances $N(1440)$, $N(1520)$, and $N(1535)$ are expected to give important contributions. We also included other potential resonances in the calculations but their partial cross sections turned out to be rather small compared to the three aforementioned ones at this energy. We therefore exclude them in the following discussion and the presentation of the results for the sake of clarity.

Effective Lagrangians treat the complex hadron bound states as pointlike particles. The non-pointlike nature of their interactions can be taken into account by the inclusion of form factors. For the purely hadronic vertices of Born contributions we choose form factors according to the scheme described in Ref. [21], which preserves gauge invariance. In Ref. [18], where the emphasis was on the angular distribution, no form factors were introduced. In the present study we use the form factors described in Ref. [21] for the $\pi N$R vertices.

For electromagnetic interactions, the pointlike case is represented by the direct photon terms and deviations from it are described by the inclusion of the intermediate $\rho$ mesons, as described above. This is equivalent to multiplying each electromagnetic vertex by a suitable form factor, the functional form of which is dominated by the Breit-Wigner propagator of the $\rho$ mesons.

The microscopic details of hadron interactions can lead to the appearance of extra phase factors at each vertex. Such phase factors have been discussed in the framework of a coupled-channel approach to meson-baryon scattering [31]. In our model, we include a phase factor as a phenomenological free parameter for the vertices describing the nucleon–$\rho$-meson decay mode of the baryon resonances in order to explore their effect on the interference between the direct-photon and $\rho$-meson contribution of each resonant

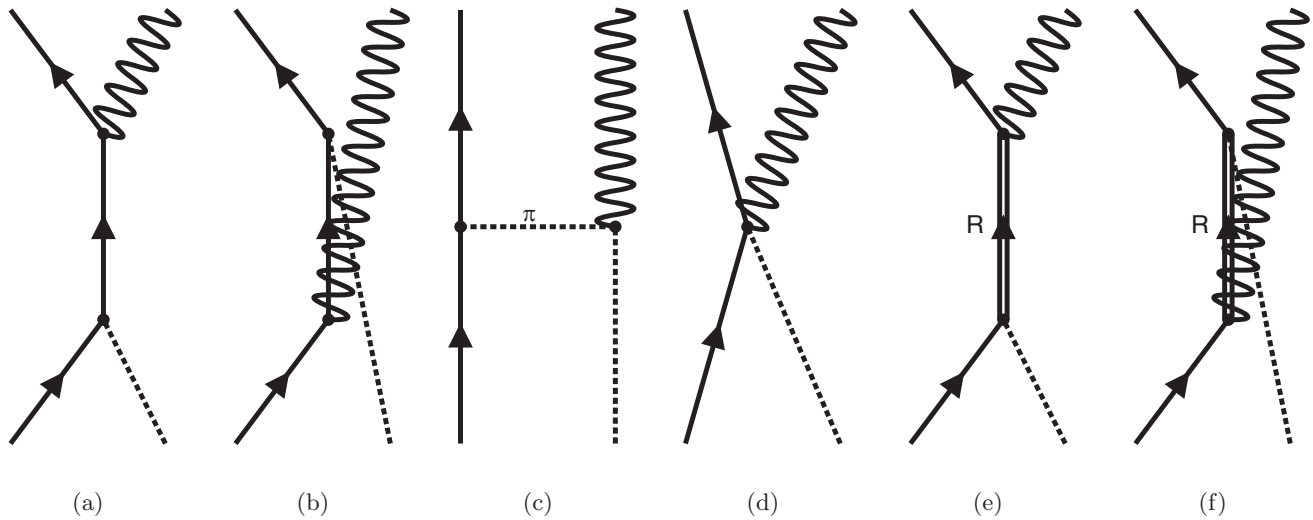


FIG. 1. Diagrams in lowest order contributing to the process $\pi^- p \to n e^+ e^-$. For clarity the emerging dilepton has been cut off in the Feynman diagrams. The wavy line is to be understood as the coherent sum of a direct photon and a photon coupled via an intermediate $\rho$ meson to the hadrons. (a)–(d) are the $s$, $u$, $t$ channels, and contact-term Born contributions, respectively. (e) and (f) show the $s$- and $u$-channel diagrams, respectively, with an intermediate baryon resonance (R).

state. This essentially means that we make the corresponding coupling constants complex via the substitution $g_{\rho NR} \to g_{\rho NR} \exp(i\phi_{\rho NR})$. This phase factor drops out when the partial decay width of resonances to the $\rho N$ final state is calculated, therefore only the moduli of the coupling constants can be determined in the way described above. The situation is different in the case of the Dalitz decay of resonances, $R \to N e^+ e^-$, where, due to an interference between the $\rho$ and direct $\gamma$ contributions, the phase factor would be relevant.

## III. RESULTS

We use the model outlined in Sec. II to study the dilepton production process in pion-nucleon collisions at the energy of recent experiments by the HADES collaboration, $\sqrt{s} = 1.49$ GeV. In this energy range, the nearby $N(1520)$ resonance is expected to strongly contribute to dilepton production due to its strong coupling to the $\rho$ meson. In Fig. 2 we show the $s$-channel $N(1520)$ contribution to the differential cross section $d\sigma/dm_{\rm inv}$ as a function of the dilepton invariant mass $m_{\rm inv}$. If we do not include any extra relative phase between the direct photon and the $\rho$-meson contributions then we experience a constructive interference resulting in a smooth invariant-mass spectrum. The maximum at $m_{\rm inv} \approx 0.5$ GeV is due to the $\rho$-meson contribution. The introduction of the extra phase in the $\rho$-meson contribution changes the interference pattern, and for $\phi_{\rho NR} = 180^\circ$ a deep minimum appears above $m_{\rm inv} = 0.4$ GeV.

Figure 3 represents our model's prediction for the differential cross section $d\sigma/dm_{\rm inv}$ of the reaction $\pi^- p \to N e^+ e^-$ at $\sqrt{s} = 1.49$ GeV c.m. energy as a function of the invariant mass $m_{\rm inv}$. The largest contributions are shown, i.e., those of the Born terms and of the baryon resonances $N(1520)$, $N(1535)$, and $N(1440)$. For the resonant contributions we indicate the uncertainties arising from the errors on the resonance widths and branching ratios. Furthermore, we show the results obtained with two different assumptions on the extra phase of the resonance-$\rho$ contributions: with no extra phase factor, and with a common phase of $\phi_{\rho NR} = 180^\circ$ at all $\rho NR$ vertices.

Comparing the two plots we see that the above extra phase factor influences both the shape and the magnitude of the differential cross section for invariant masses above 0.3 GeV. In the coupled-channel model of Ref. [31] relative phases of scattering amplitudes have been extracted. For instance, for the $\pi N \to N(1520) \to N\rho$ amplitude, a phase of $\phi_{\pi\rho}^{N(1520)} = -7.0^\circ$ was obtained. This factor is, however, a product of the phases corresponding to the $\pi NN(1520)$ and $\rho NN(1520)$

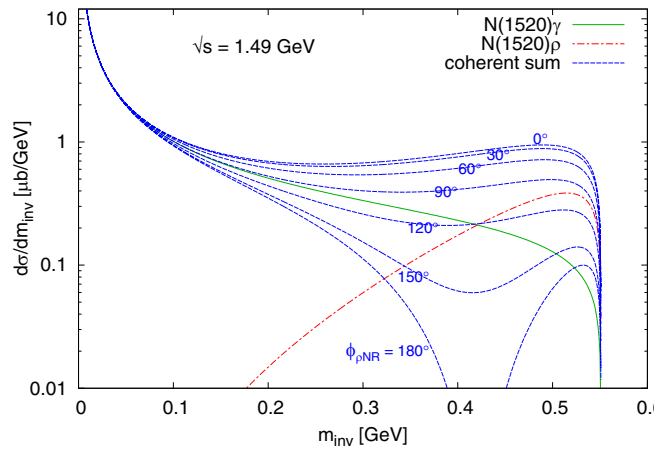


FIG. 2. Contributions with an $N(1520)$ resonance in the $s$ channel to the differential cross section $d\sigma/dm_{\rm inv}$ of dilepton production. Two of the lines indicate the direct-photon and the $\rho$-meson contributions. The other curves show the coherent sum of the above two, assuming different relative phases.

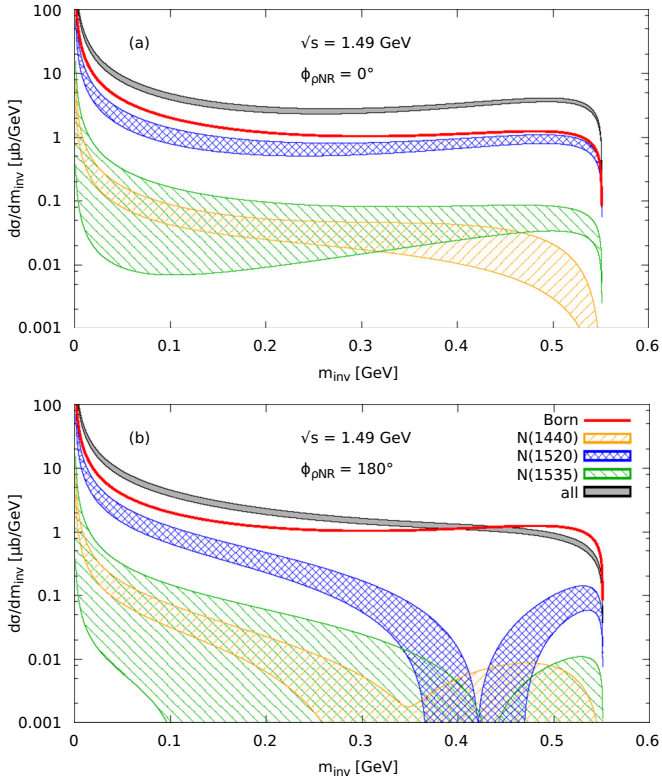


FIG. 3. Differential cross section $d\sigma/dm_{\rm inv}$ of the process $\pi^- p \to n e^+ e^-$ at c.m. energy $\sqrt{s} = 1.49\,\text{GeV}$, with no extra phase factor (a), and with a common phase factor of $\phi_{\rho NR} = 180^\circ$ (b) introduced in the $\rho N$R vertices. The legend for line styles and fill bands of the lower plot is valid for the upper plot too. The size of each band corresponds to the uncertainty on the width and branching ratio of the resonance as shown in Table I.

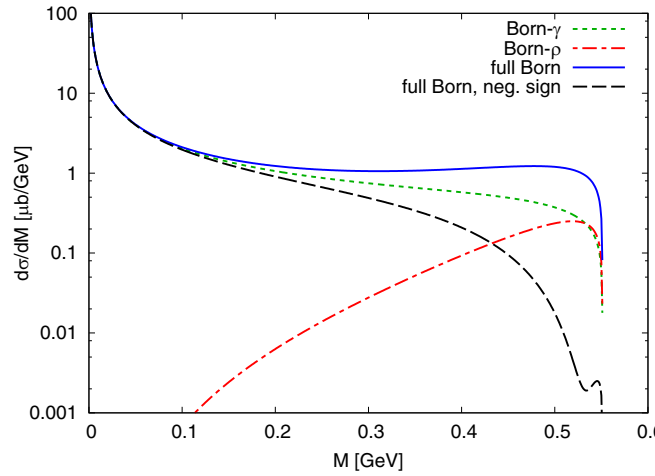


FIG. 4. Born contributions to the differential cross section $d\sigma/dm_{\rm inv}$ of the process $\pi^- p \to n e^+ e^-$ at c.m. energy $\sqrt{s} = 1.49\,\text{GeV}$, within the model described in this paper (solid line) and with an extra minus sign introduced in all interaction terms involving a $\rho$ meson (dashed line).

vertices, while the individual phase factors cannot be extracted. As already pointed out, we therefore treat the phase factors at the $\rho N$R vertices as free parameters. In principle, these phases can be different for each baryon resonance. For simplicity, we always use a common value for all resonances in this article. However, since by far the most important resonance contributions are due to the $N(1520)$, relative phases for the other resonances would have only minor effects.

Figure 3 shows also the significance of the various contributions. Independent of the phase factor, the Born terms and the $N(1520)$ provide the largest contributions. In the $\phi_{\rho NR} = 0^\circ$ case, the $N(1520)$ is almost as strong as the Born contribution at the large invariant mass end of the spectrum, due to its strong coupling to the $\rho$ meson. Integrating the cross section over the $m_{\rm inv} > 0.3\,\text{GeV}$ region where the contribution of the $\rho$ meson is significant, we obtain $\sigma(m_{\rm inv} > 0.3\,\text{GeV}) = \int_{>0.3\,\text{GeV}} (d\sigma/dm_{\rm inv}) dm_{\rm inv} = 0.73\,\mu\text{b}$, which is a result of a contribution of $0.28\,\mu$b from Born terms, $0.17\,\mu$b from $N(1520)$ terms and $0.28\,\mu$b from Born-$N(1520)$ interference. Contributions of the other two resonances are at least an order of magnitude smaller. In the $\phi_{\rho NR} = 180^\circ$ case the $N(1520)$ contribution shows a minimum around $m_{\rm inv} \approx 0.4\,\text{GeV}$ and becomes negligible compared to the Born term.

In Ref. [21] no attempt was made to determine the signs of hadron-$\rho$ interactions, only the signs of $\gamma N$R Lagrangians were varied in such a way that the best description of pion-photoproduction cross-sections are achieved. In fact, both for the Born terms and for the $N(1520)$ contributions, a destructive interference occurred between the photon and the $\rho$-meson contributions due to the choices of signs in the relevant terms of the Lagrangian. In terms of the present model, this scenario would correspond to setting $\phi_{\rho NR} = 180^\circ$ and including an extra minus sign in the $\rho NN$, $\pi\rho NN$, and $\pi\pi\rho$ vertices. In Fig. 4 we show the interference effects on the invariant-mass spectrum in the Born contributions. Dotted and dash-dotted lines correspond to the Born-$\gamma$ and Born-$\rho$ contributions, the continuous line depicts the full Born contribution according to the model used in the present paper while the dashed line shows the full Born contribution obtained with an extra minus sign introduced in the Born-$\rho$ term. In the latter case the Born contribution is strongly reduced for large invariant masses due to the destructive interference.

In Fig. 5 we show the differential cross-section $d\sigma/dm_{\rm inv}$ of the process $\pi^- p \to n e^+ e^-$ at c.m. energy $\sqrt{s} = 1.49\,\text{GeV}$ as obtained from the modified model with $\phi_{\rho NR} = 180^\circ$ and an extra minus sign in the Born-$\rho$ contribution. In this version, the signs of interaction Lagrangians are analogous to the model of Ref. [21]. However, the Lagrangians describing interactions of baryon resonances are different in the present model, and in the determination of coupling constants involving baryon resonances we used updated values for their masses and widths. Due to the destructive interference, the Born contribution is suppressed for high invariant mass and the $N(1520)$ becomes dominant. As a result, the minimum in the $N(1520)$ contribution is visible even after coherently summing all contributions. The resulting invariant mass spectrum is very similar to the one shown in Ref. [21].

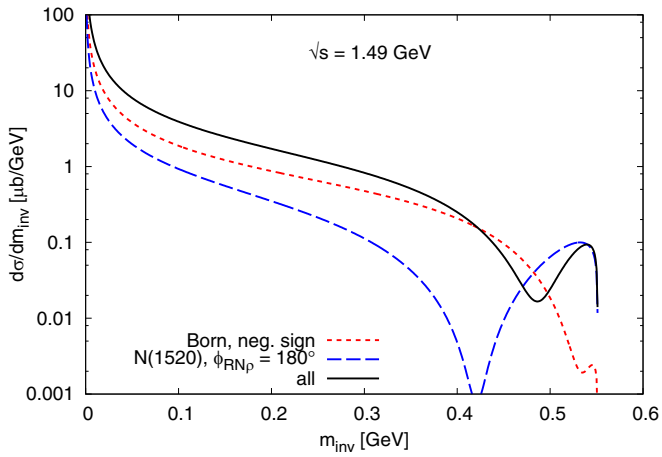


FIG. 5. Differential cross section $d\sigma/dm_{\rm inv}$ of the process $\pi^- p \to n e^+ e^-$ at c.m. energy $\sqrt{s} = 1.49\,\text{GeV}$, within the model modified in such a way that destructive interference occurs between the photon and $\rho$-meson contributions in the case of both the resonance and the Born terms.

In the following we assume no extra minus sign in the Born-$\rho$ contribution and we regard $\phi_{\rho N\rm R} = 0^\circ$ as the standard value. These choices are suggested by the arguments of Sec. II B based on the equivalence of the two versions of VMD, and they were used in the upper plot of Fig. 3. We, however, still explore the effects of a nonzero $\phi_{\rho N\rm R}$ phase factor.

In Ref. [18], the angular distribution of dileptons was discussed in terms of the anisotropy coefficient $\lambda_\theta$ and it was discussed how this and other similar coefficients are related to the polarization of the virtual photon. However, the hadronic spin density matrix, $\rho^{\rm had}_{\lambda,\lambda'}$, is itself an object representing the virtual-photon polarization state. According to Eq. 5, elements of this density matrix could in principle be determined based on the experimentally observed angular distribution of dileptons if sufficient statistics is available.

We used our model to give numerical predictions for the density matrix elements $\rho^{\rm had}_{1,1}$, $\rho^{\rm had}_{1,0}$, and $\rho^{\rm had}_{1,-1}$. Figure 6 shows these matrix elements as a function of the scattering angle $\theta_{\gamma^*}$. We present the results obtained from the two most important contributions: the Born terms (a) and the $s$-channel $N(1520)$ diagram (b). At the bottom the combined result of the above two are shown for the two cases where no extra phase factor is assumed between the direct-$\gamma$ and the $\rho$-meson contributions of the $N(1520)$ (c) and a phase factor of $\phi_{\rho N\rm R} = 180^\circ$ is included (d). For each matrix element, three different curves are plotted assuming three different values for the invariant mass $m_{\rm inv}$. On the plots one can follow how the shape of the curves is influenced by the relative strength of the two dominant contributions for various invariant masses.

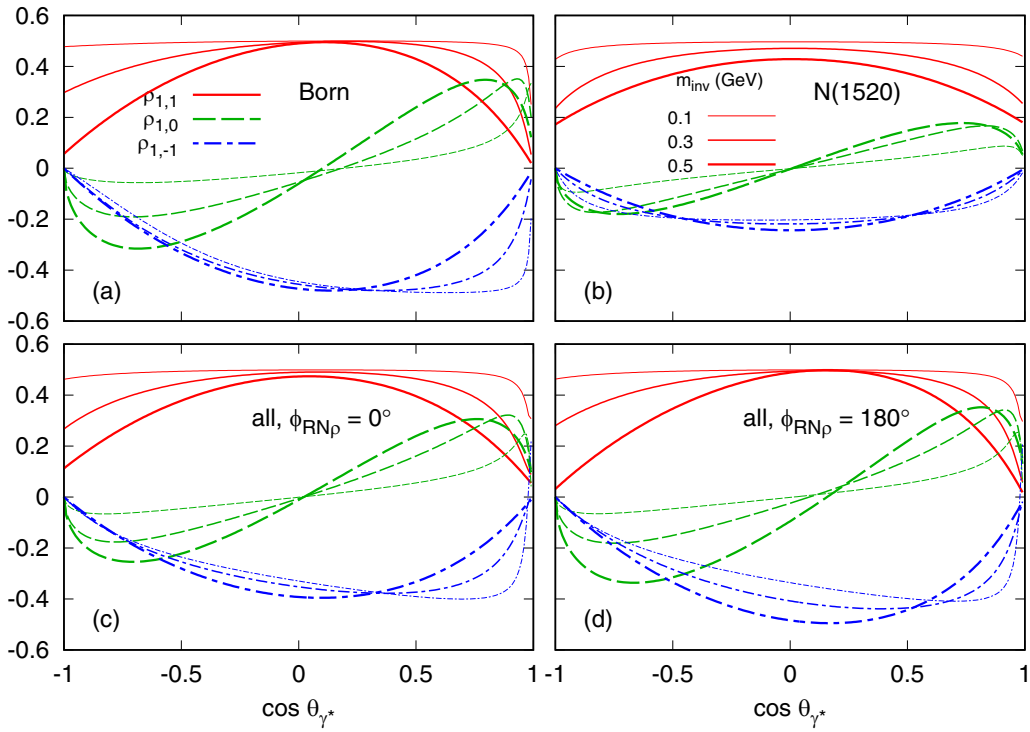


FIG. 6. Hadronic density-matrix elements $\rho_{1,1}$ (solid lines), $\rho_{1,0}$ (dashed lines), and $\rho_{1,-1}$ (dash-dotted lines) obtained from the Born contributions (a), the $N(1520)$ resonance contributions (b), and the coherent sum of the above two assuming no extra phase factor between the $N(1520)$-direct $\gamma$ and $N(1520)$-$\rho$ meson terms (c), and assuming a phase factor of $\phi_{\rho N\rm R} = 180^\circ$ (d). The lines in each set correspond to virtual photon masses $m_{\rm inv} = 0.1$ (thinnest), 0.3, and 0.5 GeV (thickest).

## IV. CONCLUSIONS AND OUTLOOK

We have presented a model study of the dilepton production process in pion-nucleon collisions in the second resonance region. The applied effective-Lagrangian model is based on the earlier works of [21] and [18]. We calculated both the contributions of baryon resonances and the nonresonant (Born) terms. For the electromagnetic interaction of hadrons, we employed a version of the vector-meson dominance (VMD) model in which hadrons couple to the electromagnetic field both directly and via an intermediate $\rho$ meson. For the interaction Lagrangians involving higher-spin resonances we used a consistent interaction scheme eliminating lower-spin degrees of freedom. We fixed the relative signs of hadron-photon and hadron-$\rho$ interaction Lagrangians based on the requirement that in the limit of universal coupling constants, the VMD model used in the present study should become equivalent to the other standard form of VMD.

We carried out numerical calculations for $\sqrt{s} = 1.49\,\text{GeV}$ c.m. energy, which coincides with the energy of recent experiments by the HADES collaboration. The $N\rho$ coupling strengths of the baryon resonances relevant at this energy have been determined using the corresponding branching ratios that were obtained from results of the same HADES experiment on pion pair production [20].

We presented our model predictions for the differential cross section $d\sigma/dm_{\text{inv}}$ and indicated the uncertainties arising from the insufficient knowledge of the widths and branching ratios of baryon resonances. Our results show that at this energy the Born terms and the term with an $s$-channel $N(1520)$ resonance give the most significant contributions. In the present calculation the $N(1440)$ contribution is smaller than in the model of Ref. [18], due to the very small upper limit for the $N\rho$ branching ratio of $N(1440)$ found in Ref. [20].

We demonstrated how the introduction of a phenomenological phase factor for the resonance-nucleon-$\rho$ vertices influences the shape of the invariant mass spectrum. While the overall effect on the cross section still depends on the individual magnitudes of the respective channels, the phase factor determines how constructive or destructive the interference between the different contributions is. In particular, we have shown that in the absence of such a phase factor there is a constructive interference between the direct-photon and the $\rho$-meson contributions of baryon resonances. A phase factor of $180^\circ$ results in a destructive interference and a minimum appears in the invariant mass spectrum around $m_{\text{inv}} = 0.4\,\text{GeV}$. A similar minimum has been seen also in [21] where a different choice was made for the signs of interaction Lagrangians involving a $\rho$ meson.

We presented predictions for elements of the spin density matrix $\rho^{\text{had}}_{\lambda,\lambda'}$, which represents the polarization state of the intermediate virtual photon. The density-matrix elements are given as a function of the scattering angle for various fixed values of the invariant mass. These matrix elements can in principle be determined from the angular distribution of dileptons originating from the decay of the virtual photon. However, for this the measurement of a multi-differential cross section is needed with sufficient statistics: for each fixed value of the invariant mass $m_{\text{inv}}$ and scattering angle $\theta_{\gamma^*}$, the dependence of the differential cross section on the electron angles $\theta_e$ and $\phi_e$ will determine the density matrix elements.

For high invariant masses ($m_{\text{inv}} \gtrsim 0.45\,\text{GeV}$), diagrams involving an intermediate $\rho$ meson à la VMD dominate over the ones containing a direct coupling to the photon, as demonstrated for the case of $N(1520)$ contributions in Fig. 2. The intermediate $\rho$ meson is in the same polarization state as the virtual photon it converts to. Predominantly $\rho$ mesons decay into a pion pair, therefore the intermediate $\rho$ meson can be studied via the $\pi^- p \to n\pi^+\pi^-$ reaction. In particular, the polarization state and the spin density matrix of the $\rho$ meson might be accessible via the angular distribution of the produced pion pair. Such an analysis assumes that the $\rho$-meson contribution to pion pair production can be disentangled from other contributions.

For low invariant masses, diagrams with direct coupling to the photon are dominant. These ingredients of the model can be independently tested in processes involving real photons, e.g., photoproduction experiments.

In dilepton production, both hadron-$\rho$ and direct hadron-photon couplings play a role, therefore the interference of these two contributions and in particular their relative phase can be studied. High statistics dilepton spectra obtainable in pion-beam experiments by HADES could provide an ideal test environment for the above effects and the present, or other similar models.

To study properties of baryon resonances in the third resonance region the HADES collaboration will continue the experimental campaign using a secondary pion beam at the c.m. energy of $\sqrt{s} = 1.76\,\text{GeV}$ [33], serving as a precursor for current and future meson beam facilities for baryon spectroscopy [34,35]. At this energy we expect the spin-5/2 resonances $N(1680)$ and $N(1675)$ to contribute to the cross section. This will most easily be visible via a different dependence of spin density matrix elements on the scattering angle $\theta_{\gamma^*}$. Our model already includes relevant resonances for the third resonance region and can easily be extended to include missing ones. Preliminary calculations show that different choices of form factors will result in more significant differences at higher energies, therefore a careful study of their effects will be necessary. Possible approaches to the electromagnetic form factor of hadrons relevant for higher energies include the extended vector-meson dominance model of Ref. [36], where excited $\rho$-meson states are also included, or the microscopic model of Refs. [15–17], where electromagnetic interaction of hadrons is described as a sum of valence-quark and pion-cloud contributions.

## ACKNOWLEDGMENTS

We would like to thank Bengt Friman, Béatrice Ramstein, Piotr Salabura, Enrico Speranza, and Joachim Stroth for valuable discussions. D.N. was supported by the GSI F&E. M.B., T.G., and D.N. acknowledge support by the Deutsche Forschungsgemeinschaft (DFG, German Research Foundation) through the CRC-TR 211 'Strong-interaction matter under extreme conditions', Project No. 315477589 - TRR 211. M.Z. was supported by the Hungarian

NKFIH Grant No. 2019-2.1.6-NEMZ_KI-2019-00001, by COST Action CA15213 "Theory of hot matter and relativistic heavy-ion collisions" (THOR), the CREMLINplus project, and the Helmholtz Alliance HA216/EMMI.

## APPENDIX A: LAGRANGIANS

For the Born terms, i.e., the nonresonant contributions, we chose the same Lagrangians as Ref. [21]. We use a pseudovector nucleon-pion coupling of the form

$$\mathscr{L}_{\pi NN} = -\frac{f_{\pi NN}}{m_\pi}\overline{\psi}_N\gamma_5\gamma^\mu\vec{\tau}\psi_N\cdot\partial_\mu\vec{\pi}, \tag{A1}$$

where $\vec{\tau} = (\tau_1, \tau_2, \tau_3)$ are the Pauli matrices in isospin space and $f_{\pi NN} = 0.97$ is a coupling constant where the value is taken from Ref. [37]. The direct coupling of the nucleon and the pion to the photon is given by the interaction terms

$$\mathscr{L}_{\gamma NN} = -e\overline{\psi}_N\left[\frac{1+\tau_3}{2}\not{A} - \left(\frac{1+\tau_3}{2}\kappa_p + \frac{1-\tau_3}{2}\kappa_n\right)\frac{\sigma_{\mu\nu}}{4m_N}F^{\mu\nu}\right]\psi_N, \tag{A2}$$

$$\mathscr{L}_{\gamma\pi\pi} = -ieA_\mu(\pi^-\partial^\mu\pi^+ - \pi^+\partial^\mu\pi^-), \tag{A3}$$

where the anomalous magnetic moments of the proton and the neutron are $\kappa_p = 1.793$, $\kappa_n = -1.913$. The interaction of the nucleon and the pion with the $\rho$ meson is described by Lagrangians analogous to the above two,

$$\mathscr{L}_{\rho NN} = -\frac{\tilde{g}_\rho}{2}\overline{\psi}_N\left(\not{\vec{\rho}} - \kappa_\rho\frac{\sigma_{\mu\nu}}{4m_N}\vec{\rho}^{\mu\nu}\right)\vec{\tau}\psi_N, \tag{A4}$$

$$\mathscr{L}_{\rho\pi\pi} = -\tilde{g}_\rho[(\partial^\mu\vec{\pi})\times\vec{\pi}]\vec{\rho}_\mu, \tag{A5}$$

where a value of $\tilde{g}_\rho = 5.96$ is obtained from the width of the $\rho\to\pi\pi$ decay. For the tensor coupling, $\kappa_\rho$, values between 1.99 and 2.65 have been obtained in Ref. [38] based on various PWA solutions. Here, we use $\kappa_\rho = 2.3$. The presence of the derivative of the pion field in the nucleon-pion interaction, Eq. (A1) forces us to introduce four-point interactions of the form

$$\mathscr{L}_{\gamma\pi NN} = -\frac{ief_{\pi NN}}{m_\pi}\overline{\psi}_N\gamma_5\gamma^\mu\vec{\tau}\psi A_\mu Q\vec{\pi}, \tag{A6}$$

$$\mathscr{L}_{\rho\pi NN} = -\frac{\tilde{g}_\rho f_{\pi NN}}{m_\pi}\overline{\psi}_N\gamma_5\gamma^\mu\vec{\tau}\psi(\vec{\rho}_\mu\times\vec{\pi}) \tag{A7}$$

in order to maintain gauge invariance.

In the present model we describe the baryon resonance transition vertices by the same Lagrangians as in Ref. [18], but we also include direct coupling terms to the photon, using forms analogous to the corresponding interaction Lagrangians with the $\rho$ meson. For higher-spin resonances we employ the consistent interaction scheme of Ref. [22]. The interaction Lagrangians involving spin-1/2 and spin-3/2 resonances are given by

$$\mathscr{L}_{\pi NR_{1/2}} = -\frac{2g_{\pi NR}}{m_\pi}\overline{\psi}_R\Gamma\gamma^\mu\vec{\mathcal{T}}\psi_N\partial_\mu\vec{\pi} + \text{H.c.}, \tag{A8}$$

$$\mathscr{L}_{\pi NR_{3/2}} = i\frac{2g_{\pi NR}}{m_\pi^2}\overline{\Psi}^\mu_R\Gamma\vec{\mathcal{T}}\psi_N\partial_\mu\vec{\pi} + \text{H.c.}, \tag{A9}$$

$$\mathscr{L}_{\rho NR_{1/2}} = \frac{g_{\rho NR}}{m_\rho}\overline{\psi}_R\vec{\mathcal{T}}\sigma^{\mu\nu}\tilde{\Gamma}\psi_N\vec{\rho}_{\mu\nu} + \text{H.c.}, \tag{A10}$$

$$\mathscr{L}_{\rho NR_{3/2}} = -i\frac{g_{\rho NR}}{2m_\rho^2}\overline{\Psi}^\mu_R\vec{\mathcal{T}}\gamma^\nu\tilde{\Gamma}\psi_N\vec{\rho}_{\mu\nu} + \text{H.c.}, \tag{A11}$$

$$\mathscr{L}_{\gamma NR_{1/2}} = -\frac{g_{\gamma NR}}{2m_\rho}\overline{\psi}_R\sigma^{\mu\nu}\tilde{\Gamma}\psi_N F_{\mu\nu} + \text{H.c.}, \tag{A12}$$

$$\mathscr{L}_{\gamma NR_{3/2}} = i\frac{g_{\gamma NR}}{4m_\rho^2}\overline{\Psi}^\mu_R\gamma^\nu\tilde{\Gamma}\psi_N F_{\mu\nu} + \text{H.c.}, \tag{A13}$$

where $R_J$ corresponds to a baryon resonance with total spin $J$. $\Gamma = \gamma^5$ if $J^P \in \{1/2^+, 3/2^-\}$ and $\Gamma = 1$ otherwise, and $\tilde{\Gamma} = \gamma^5\Gamma$. $\vec{\mathcal{T}} = \vec{\tau}/2$ if the baryon resonance has a total isospin equal to 1/2 (R = $N^*$), while $\vec{\mathcal{T}} = \vec{\Theta}$ in case of an isospin-3/2 resonance (R = $\Delta^*$). Here $\vec{\Theta} = (\Theta_1, \Theta_2, \Theta_3)$ are the isospin 1/2 to 3/2 transition matrices.

In line with the consistent scheme of Ref. [22], spin-3/2 baryons are represented by the field

$$\Psi_\mu = i\gamma^\nu(\partial_\mu\psi_\nu - \partial_\nu\psi_\mu), \tag{A14}$$

where $\psi_\mu$ is the traditional Rarita-Schwinger field.

The propagators for the spin-1/2 particles are given by

$$S_{1/2} = \frac{i}{p_R^2 - m_R^2 + i\sqrt{p_R^2}\Gamma_R}(\not{p}_R + m_R) \tag{A15}$$

and those for the spin-3/2 particles by

$$S^{\mu\nu}_{3/2} = \frac{i}{p_R^2 - m_R^2 + i\sqrt{p_R^2}\Gamma_R(p_R^2)}P^{\mu\nu}_{3/2}(p_R, m_R) \tag{A16}$$

with the projector

$$P^{\mu\nu}_{3/2} = -(\not{p}_R + m_R)\left(g^{\mu\nu} - \frac{\gamma^\mu\gamma^\nu}{3}\right). \tag{A17}$$

Terms in the projectors that are proportional to $p_R^\mu$ have been neglected since they cancel out when contracted with the vertices. The general expression can be found in Ref. [21]. Furthermore we use the same width parametrization for baryon resonances as in Ref. [21].

## APPENDIX B: COUPLING CONSTANTS

We took the Breit-Wigner mass $m$ and total decay width $\Gamma$ of baryon resonances from the Review of Particle Physics [32] by the Particle Data Group (PDG). The PDG provides an upper ($u$) and lower ($l$) value for the total widths of

resonances and their branching ratios (BR) to the $N\pi$ and $N\gamma$ final state. We used $\mathrm{BR} = \frac{u+l}{2} \pm \frac{u-l}{2}$ for the mean value and the uncertainty of the branching ratios and a similar expression for the total widths. Using these we obtain the partial widths and their uncertainties. The values and uncertainties of the corresponding coupling constants are determined by requiring that our model's prediction for the partial widths reproduces the PDG values and uncertainties.

Using a partial-wave analysis of the reaction $\pi^- p \to N\pi\pi$, the HADES experiment reported for the branching ratios of $N(1520)$ and $N(1535)$ to the $N\rho$ final state the values $(12.2 \pm 1.9)\%$ and $(3.2 \pm 0.7)\%$, respectively [20], while for the $N(1440)$ an upper limit of 0.2% was obtained, which we interpret as $(0.1 \pm 0.1)\%$. The coupling strength of the resonance to the $N\rho$ channel can be determined based on the decay mode $\mathrm{R} \to N\rho \to N\pi\pi$. From the effective-Lagrangian model one can obtain the prediction for this decay width via integration over the $\rho$-meson spectral function according to

$$\begin{aligned}\Gamma_{\mathrm{R}\to N\pi\pi(\rho)} &= \Gamma_{\mathrm{R}\to N\rho} \\ &= \frac{1}{4\pi^2}\int dm_{\mathrm{inv}}\frac{|\mathbf{p}_N|}{m_{\mathrm{R}}^2}\frac{1}{n_{\mathrm{pol,R}}}\sum|\mathcal{M}_{\mathrm{R}\to N\rho}|^2 \\ &\quad\times\frac{m_{\mathrm{inv}}^2\Gamma_\rho(m_{\mathrm{inv}})}{\left(m_{\mathrm{inv}}^2-m_\rho^2\right)^2+m_{\mathrm{inv}}^2\Gamma_\rho(m_{\mathrm{inv}})^2},\end{aligned} \tag{B1}$$

where we have taken into account that the $\rho$ meson decays to a pion pair with ≈100% branching ratio. The $\rho N\mathrm{R}$ coupling constants and their uncertainties are determined by requiring that the model reproduces the $N\rho$ partial widths obtained by combining the total width given by PDG and experimental $N\rho$ branching ratio by HADES. The coupling constants of baryon resonances are summarized in Table I.


[1] R. Rapp, J. Wambach, and H. van Hees, The chiral restoration transition of QCD and low mass Dileptons, in *Relativistic Heavy Ion Physics*, edited by R. Stock, Landolt Bornstein, New Series I/23A (Springer, Berlin, 2010), Sec. 4.1.

[2] C. Gale, Photon production in hot and dense strongly interacting matter, in *Relativistic Heavy Ion Physics*, edited by R. Stock, Landolt Bornstein, New Series I/23A (Springer, Berlin, 2010), Sec. 6.3.

[3] R. Rapp and H. van Hees, Thermal dileptons as fireball thermometer and chronometer, Phys. Lett. B **753**, 586 (2016).

[4] J. Adamczewski-Musch *et al.* (Hades Collaboration), Probing dense baryon-rich matter with virtual photons, Nat. Phys. **15**, 1040 (2019).

[5] R. Arnaldi *et al.* (NA60 Collaboration), First Measurement of the Rho Spectral Function in High-Energy Nuclear Collisions, Phys. Rev. Lett. **96**, 162302 (2006).

[6] D. Adamova *et al.* (CERES Collaboration), Modification of the rho-meson detected by low-mass electron-positron pairs in central Pb-Au collisions at 158-A-GeV/c, Phys. Lett. B **666**, 425 (2008).

[7] M. Makek (PHENIX Collaboration), PHENIX results on low-mass dileptons in Au + Au collisions with the Hadron Blind Detector, Nucl. Phys. A **956**, 425 (2016).

[8] S. Acharya *et al.* (ALICE Collaboration), Measurement of dielectron production in central Pb-Pb collisions at $\sqrt{s_{\mathrm{NN}}} = 2.76$ TeV, Phys. Rev. C **99**, 024002 (2019).

[9] M. Herrmann, B. Friman, and W. Norenberg, Properties of rho mesons in nuclear matter, Nucl. Phys. A **560**, 411 (1993).

[10] G. Chanfray and P. Schuck, The rho meson in dense matter and its influence on dilepton production rates, Nucl. Phys. A **555**, 329 (1993).

[11] W. Peters, M. Post, H. Lenske, S. Leupold, and U. Mosel, The spectral function of the rho meson in nuclear matter, Nucl. Phys. A **632**, 109 (1998).

[12] G. Chanfray, R. Rapp, and J. Wambach, Medium Modifications of the Rho Meson at CERN SPS Energies, Phys. Rev. Lett. **76**, 368 (1996).

[13] D. Cabrera, E. Oset, and M. Vicente Vacas, Chiral approach to the rho meson in nuclear matter, Nucl. Phys. A **705**, 90 (2002).

[14] R. Rapp, Theory of soft electromagnetic emission in heavy-ion collisions, Acta Phys. Pol. B **42**, 2823 (2011).

[15] G. Ramalho, M. T. Peña, J. Weil, H. van Hees, and U. Mosel, Role of the pion electromagnetic form factor in the $\Delta(1232) \to \gamma^* N$ timelike transition, Phys. Rev. D **93**, 033004 (2016).

[16] G. Ramalho and M. T. Peña, $\gamma^*\mathrm{N}\to\mathrm{N}^*(1520)$ form factors in the timelike regime, Phys. Rev. D **95**, 014003 (2017).

[17] G. Ramalho and M. T. Peña, Covariant model for the Dalitz decay of the $N(1535)$ resonance, Phys. Rev. D **101**, 114008 (2020).

[18] E. Speranza, M. Zétényi, and B. Friman, Polarization and dilepton anisotropy in pion-nucleon collisions, Phys. Lett. B **764**, 282 (2017).

[19] J. J. Sakurai, Theory of strong interactions, Ann. Phys. (NY) **11**, 1 (1960).

[20] J. Adamczewski-Musch *et al.* (HADES Collaboration), Two-pion production in the second resonance region in $\pi^- p$ collisions with HADES, Phys. Rev. C **102**, 024001 (2020).

[21] M. Zétényi and G. Wolf, Dilepton production in pion-nucleon collisions in an effective field theory approach, Phys. Rev. C **86**, 065209 (2012).

[22] T. Vrancx, L. De Cruz, J. Ryckebusch, and P. Vancraeyveld, Consistent interactions for high-spin fermion fields, Phys. Rev. C **84**, 045201 (2011).

[23] A. I. Titov and B. Kampfer, Isoscalar isovector interferences in $\pi N \to \mathrm{Ne}^+ e^-$ reactions as a probe of baryon resonance dynamics, Eur. Phys. J. A **12**, 217 (2001).

[24] M. F. M. Lutz, B. Friman, and M. Soyeur, Quantum interference of rho0 and omega-mesons in the $\pi N \to \mathrm{Ne}^+ e^-$ N reaction, Nucl. Phys. A **713**, 97 (2003).

[25] D. O. Riska and G. E. Brown, Nucleon resonance transition couplings to vector mesons, Nucl. Phys. A **679**, 577 (2001).

[26] E. L. Bratkovskaya, M. Schafer, W. Cassing, U. Mosel, O. V. Teryaev, and V. D. Toneev, Anisotropy of dilepton emission from nucleon-nucleon interactions, Phys. Lett. B **348**, 325 (1995).

[27] E. L. Bratkovskaya, O. V. Teryaev, and V. D. Toneev, Anisotropy of dilepton emission from nuclear collisions, Phys. Lett. B **348**, 283 (1995).

[28] J. J. Sakurai, *Currents and Mesons* (The University of Chicago Press, Chicago, 1969).

[29] N. M. Kroll, T. D. Lee, and B. Zumino, Neutral vector mesons and the hadronic electromagnetic current, Phys. Rev. **157**, 1376 (1967).

[30] H. B. O'Connell, B. Pearce, A. W. Thomas, and A. G. Williams, $\rho$-$\omega$ mixing, vector meson dominance and the pion form-factor, Prog. Part. Nucl. Phys. **39**, 201 (1997).

[31] M. Lutz, G. Wolf, and B. Friman, Scattering of vector mesons off nucleons, Nucl. Phys. A **706**, 431 (2002).

[32] M. Tanabashi *et al.* (Particle Data Group Collaboration), Review of particle physics, Phys. Rev. D **98**, 030001 (2018).

[33] J. Adamczewski-Musch *et al.* (HADES Collaboration), A facility for pion-induced nuclear reaction studies with HADES, Eur. Phys. J. A **53**, 188 (2017).

[34] W. J. Briscoe, M. Döring, H. Haberzettl, D. M. Manley, M. Naruki, I. I. Strakovsky, and E. S. Swanson, Physics opportunities with meson beams, Eur. Phys. J. A **51**, 129 (2015).

[35] K. Hicks *et al.* (E45 Collaboration), 3-body hadronic reactions for new aspects of baryon spectroscopy, Proposal for J-PARC 50 GeV Proton Synchrotron, http://j-parc.jp/researcher/Hadron/en/pac_1207/pdf/P45_2012-3.pdf (2012).

[36] M. Krivoruchenko, B. Martemyanov, A. Faessler, and C. Fuchs, Electromagnetic transition form-factors and dilepton decay rates of nucleon resonances, Ann. Phys. (NY) **296**, 299 (2002).

[37] H. Garcilazo and E. de Guerra, A model for pion electro- and photo-production from threshold up to 1 GeV, Nucl. Phys. A **562**, 521 (1993).

[38] T. Feuster and U. Mosel, A Unitary model for meson nucleon scattering, Phys. Rev. C **58**, 457 (1998).